$1s2s2p^2 3s\ ^6P - 1s2p^3 3s\ ^6S^o$ Transitions in O IV

Bin Lin,[1,*] H. Gordon Berry,[1,†] Tomohiro Shibata,[1] A. Eugene Livingston,[1] Henri-Pierre Garnir,[2] Thierry Bastin,[2] J. Désesquelles,[3] and Igor Savukov[1]

[1]*Department of Physics, University of Notre Dame, Notre Dame, Indiana 46556, USA*

[2]*IPNAS, University of Liege, B4000 Liege, Belgium*

[3]*Lab Spectrometrie Ion & Mol, University of Lyon 1, F-69622 Villeurbanne, France*

(Received 8 January 2003; published 26 June 2003)

The energies and lifetimes of doubly excited sextet states of boron-like O IV, F V, and Ne VI are calculated with the multiconfiguration Hartree-Fock approach, including QED and higher-order corrections, and also with the multiconfiguration Dirac-Fock GRASP code. The wavelengths and transition rates of electric-dipole transitions from the inner-shell excited terms $1s2s2p^2 3s\ ^6P - 1s2p^3 3s\ ^6S^o$ are investigated by beam-foil spectroscopy in the XUV spectral region. The predicted transition wavelengths agree with the experiment. The higher-order corrections, fine structures, and spectrum with high wavelength resolution are found to be critically important in these comparisons. Nine new lines have been identified. The ground sextet states of boronlike atoms are metastable and well above several ionization levels. These are possible candidates for XUV and soft x-ray lasers.

DOI: 10.1103/PhysRevA.67.062507 PACS number(s): 32.70.−n, 39.30.+w

I. INTRODUCTION

All the atomic energy levels where only a single electron is excited from the ground state are below the first ionization limit of the atomic ion being studied. In the early 1970s, the technique of fast beam spectroscopy enabled the efficient study of atomic states with more than one electron excited. These multiexcited states typically have energies well above the first ionization limit, and most such states decay very rapidly (in about 10^{-14} s) by emitting an electron, and leaving the atom ionized (in the case of an ion, with a charge one unit higher). However, the doubly excited sextet states of boronlike atoms are metastable against dipole-radiation decay to singly excited five-electron states and against autoionization decay to singly excited four-electron states [1]. The lifetimes for the lowest sextet states of boronlike O IV are about 10^{-6} s, and the higher-lying states have typically 10^{-10} s lifetimes. Such highly excited and relatively long-lived states are of interest in the production of XUV- and soft x-ray lasers.

In Fig. 1, we show an overview of excitation energies of several ionization stages above the ground state of the five-electron oxygen ion. The level structures of other isoelectronic ions (such as F V and Ne VI) are similar, and their energies scale according to their nuclear charges. The sextet levels of O IV have very high energies, principally due to the $1s$ and $2s$ electron vacancies (such atoms have been termed ''hollow atoms''). These five-electron high-spin states have energies typically just below the two-electron O VII $1s2s$ and $1s2p$ states, about 0.8 keV above the O IV ground state. The same configurations also yield quartet and doublet states, which can provide rapid x-ray emission (energies of the order of 0.8 keV in oxygen). The x-ray emission will compete with auger-electron processes, but will tend to dominate more for the more highly charged ions of the isoelectronic sequence.

The recent work of Lapierre and Knystautas [2] on possible sextet transitions in Ne VI highlights the significance and difficulties in this sequence. They obtained the very best resolution ever achieved in a beam-foil spectrum in the grazing incidence region, but their tentative identifications of the two transitions at 12.0 and 10.6 nm show rather weak lines and overwhelming blending problems. The work of Blanke *et al.* [1] in searching for the same two sextet transitions in N III, O IV and F V indicates blending problems in all six

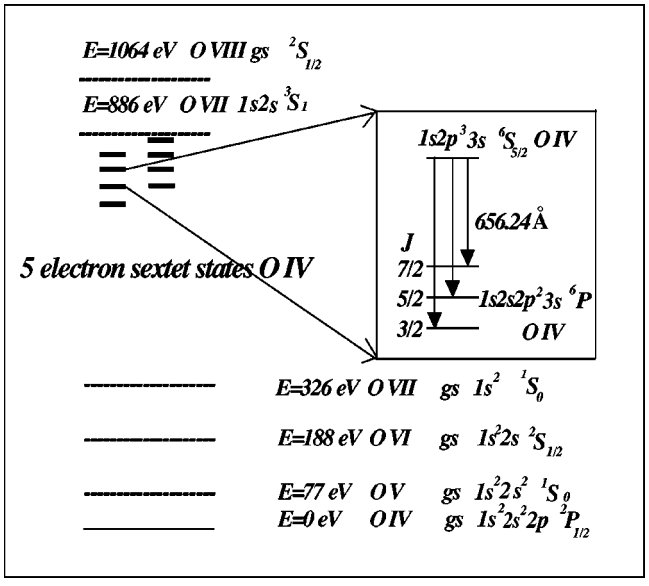

FIG. 1. Term diagram of the doubly excited sextet states of O IV. The mean wavelength for the $1s2s2p^2 3s\ ^6P_J - 1s2p^3 3s\ ^6S^o$ transitions in O IV is shown.

*Electronic address: blin@nd.edu;
URL: http://www.nd.edu/~blin/

†Electronic address: Berry.20@nd.edu;
URL: http://www.science.nd.edu/physics/Faculty/berry.html

cases. Hence, all these identifications depend sensitively on the accuracy of the various calculations. Given this uncertainty in the identification of all sextet transitions in the isoelectronic sequence, it is desirable to find unambiguous experimental verification of the calculations.

Most of the recent theoretical work on boronlike atoms has used configuration interaction (CI) methods, i.e., the multiconfiguration Hartree-Fock method (MCHF) [1,3,4], multiconfiguration Dirac-Fock method (MCDF) [1,2,5,6], or superposition of configurations Hartree-Fock relativistic method with the complex members [2]. For the sextet states in O IV, F V, and Ne VI, the CI method is still quite effective [1,3]. Hence, we can use the CI method to obtain accurate energies for the sextet states in O IV, F V, and Ne VI. The results will show the origins and sizes of the correlation energies. The CI values and energies of the sextet states depend on the configurations considered in the calculations. Generally, more configurations are better for good precision [4].

In this work, we obtain the theoretical energy and wavelength data for the doubly excited sextet states in O IV, F V, and Ne VI with the MCHF [4] and MCDF [5,6] methods. Experimentally, we rely on new results using the fast-ion beam-foil technique for O IV, and previous unpublished results for the F V and Ne VI spectra. The information from the experiments and theoretical studies greatly improves the understanding of which configurations are the most important and the origin of the correlation energies for the doubly excited sextet states in O IV, F V, and Ne VI. The results illustrate the different observation of fine structures in these states.

We are able to clarify the origin of the differences between our theoretical transition energies and the experimental data: to obtain accurate energies for the doubly excited sextet states in O IV, F V, and Ne VI, the QED effect and higher-order relativistic corrections cannot be neglected. These contributions from the QED and higher-order relativistic effects to the energy of the sextet states are calculated using the methods described below.

II. THEORY

For the calculations we use two different methods, the multiconfiguration Hartree-Fock method [4] with the QED effect and higher-order relativistic corrections, and the multiconfiguration Dirac-Fock GRASP code [5,6].

A. The multiconfiguration Hartree-Fock method with the QED effect and higher-order relativistic corrections

The energies, lifetimes and the relevant E1 transition rates of the three doubly excited sextet states $1s2s2p^3\,{}^6S^o$, $1s2s2p^2 3s\,{}^6P$, and $1s2p^3 3s\,{}^6S^o$ of boronlike O IV, F V, and Ne VI were calculated with the single-configuration Hartree-Fock (SCHF) method as well as with the multiconfiguration Hartree-Fock method. We also added calculations of the hydrogenlike QED effect and higher-order corrections.

For any sextet state in a five-electron system $(\beta, LS=5/2JM_J)=(n_1 l_1^{w1}\ n_2 l_2^{w2}\ n_3 l_3^{w3}\ n_4 l_4^{w4}\ n_5 l_5^{w5},\ {}^6L_J, M_J)$, where $wi=0,1,\ldots,2l_i-1$ for $i=1,2,\ldots,5$ and $\Sigma wi=5$, the wave function is

$$\Psi(\beta,LS=5/2J)=\sum_{i=1}^{N}\sum_{M_J=-J}^{J} c_i\phi(\beta_i,LS=5/2JM_J), \tag{1}$$

where c_i is a configuration interaction coefficient, N is the total number of configurations with the same $LSJM_J$ and parity, and $\phi\,(\beta_i,LS=5/2JM_J)$ is the configuration state function (CSF).

In the SCHF calculations, only the configurations corresponding to the desired levels were considered. After updating the MCHF codes, we performed the relativistic calculations with an initial expansion of up to 4000 CSF's and a full Pauli-Breit Hamiltonian matrix H. For a five-electron system the CI expansion generated by the active set leads to a large number of expansions. In order to reduce the number of the configurations, we chose those with the $1s$ electron singly occupied, i.e., $1sn_1l_1n_2l_2n_3l_3n_4l_4$, where $n_i=2,3,4$, and 5, $l_i=0,\ldots,\min(4,n_i-1)$. We also included $6s$ and $6p$ electrons. We did not include the g electrons for $n=5$ shell. For the MCHF calculations of the ground state $1s2s2p^3\,{}^6S^o$, we chose $1s$, $2s$, $2p$, $3s$, $3p$, $3d$, $4s$, $4p$, $4d$, $4f$, $5s$, $5p$, $5d$, $5f$, and $6s$ electrons to compose the configurations. For the $1s2s2p^2 3s\,{}^6P$ state in O IV we chose $1s$ through $5d$ electrons. For the $1s2s2p^2 3s\,{}^6P$ state in F V and Ne VI, we chose $1s$ through $5f$ electrons. For the $1s2p^3 3s\,{}^6S^o$ state in O IV we chose $1s$ through $6s$ electrons. For the $1s2p^3 3s\,{}^6S^o$ state in F V, and Ne VI we chose $1s$, $2s$, $2p$, $3s$, $3p$, $3d$, $4s$, $4p$, $4d$, $4f$, $5s$, $5p$, $5d$, $5f$, and $6p$ electrons. After determining the radial wave functions, we included the relativistic operators of mass correction, one- and two-body Darwin terms, and the spin-spin contact term. The fine-structure splitting is strongly involved in the experiments and identifications. So we included the J-dependent fine-structure operators, orbit-orbit term, spin-orbit term, and spin-other-orbit term in both SCHF(T) and MCHF(T) calculations, which were not included by Miecznik *et al.* [3].

In addition, we used the screened hydrogenic formula from Refs. [7–9] to estimate QED effect and also higher-order relativistic contributions for the sextet states in five-electron oxygen, fluorine, and neon. For an ns electron, the QED effect is

$$\Delta E_{QED}(n,0)=\frac{4Z_{eff}^4\alpha^3}{3\pi n^3}\left\{\frac{19}{30}-2\ln(\alpha Z_{eff})-\ln K(n,0)-7.214\alpha Z_{eff}-(\alpha Z_{eff})^2[3\ln^2(\alpha Z_{eff})+8.695\ln(\alpha Z_{eff})+19.081]\right\}. \tag{2}$$

For other nl electrons,

$$\Delta E_{QED}(n,l) = \frac{4Z_{eff}^4\alpha^3}{3\pi n^3}\left\{ \frac{3c_{l,j}}{8(2l+1)} - \ln K(nl) + (\alpha Z_{eff})^2 \ln(\alpha Z_{eff})^{-2} \times\left[\left(1-\frac{1}{n^2}\right)\left(\frac{1}{10}+\frac{1}{4}\delta_{j,1/2}\right)\delta_{j,l} + \frac{8[3-l(l+1)/n^2]}{(2l-1)(2l(2l+1)(2l+2)(2l+3)}\right] + \frac{3\alpha}{4\pi}(-0.3285)c_{l,j}/(2l+1)\right\}, \quad (3)$$

where

$$c_{l,j} = \begin{cases} l/(l+1) & \text{for} \quad j = 1+1/2, \\ -1/l & \text{for} \quad j = 1-1/2. \end{cases}$$

The values of $\ln K(nl)$ are taken from Drake and Swainson [9]. The effective nuclear charge Z_{eff} values are estimated as below. The energy eigenvalue of the one-electron Dirac equation for a Coulomb potential is

$$E_{Dirac}(Z) = \frac{1}{\alpha^2}\left\{1+\left[\frac{\alpha Z}{n-k+\sqrt{k^2-\alpha^2Z^2}}\right]^2\right\}^{-1/2}, \quad (4)$$

where $k = j+1$ for a hydrogenic electron. To the order of $\alpha^2 Z^4$, E_{Dirac} reduces to

$$E^{(1)}(Z) = \frac{Z^2}{2n^2}\left\{1+\frac{\alpha^2Z^2}{n}\left[\frac{1}{k}-\frac{3}{4n}\right]\right\}. \quad (5)$$

Since we have calculated the energy of the $n_5 l_5$ valence electron in the sextet state $(n_1 l_1^{w1}\, n_2 l_2^{w2}\, n_3 l_3^{w3}\, n_4 l_4^{w4}\, n_5 l_5^{w5},\ ^6L_J)$ to the order of $\alpha^2 Z^4$ with the MCHF method, we can define a Z_{eff} by

$$E_{MCHF}(n_1 l_1^{w1} n_2 l_2^{w2} n_3 l_3^{w3} n_4 l_4^{w4} n_5 l_5^{w5}, {}^6L_J) - E_{MCHF}(n_1 l_1^{w1} n_2 l_2^{w2} n_3 l_3^{w3} n_4 l_4^{w4}, {}^5L'_{J'}) = \frac{Z_{eff}^2}{2n_5^2}\left\{1+\frac{\alpha^2 Z_{eff}^2}{n_5}\left[\frac{1}{k_5}-\frac{3}{4n_5}\right]\right\}, \quad (6)$$

where $^5L'_{J'}$ is determined by the transition being studied, where the energy of the valence electron changes. Using the Z_{eff} an approximate $\Delta E_{QED}(n_5, l_5)$ in the sextet state $(n_1 l_1^{w1}\, n_2 l_2^{w2}\, n_3 l_3^{w3}\, n_4 l_4^{w4}\, n_5 l_5^{w5},\ ^6L_J)$ is estimated with Eqs. (2) and (3). With the same Z_{eff}, the higher-order relativistic correction of the electron $n_5 l_5$ is estimated from

$$\Delta E_{HO}(n_5 l_5) = E_{Dirac}(Z_{eff}) - E^{(1)}(Z_{eff}). \quad (7)$$

In the same way, we can obtain the QED effects and higher-order relativistic corrections, $\Delta E_{QED}(n_i l_i j_i, LSJ)$ and $\Delta E_{HO}(n_i l_i j_i, LSJ)$ for all five electrons $i = 1,2,\ldots,5$ in the sextet states in boronlike oxygen, fluorine, and neon. The total energy of a sextet state in O IV, F V, and Ne VI is then

$$E^T_{MCHF} = E_{MCHF}(\beta, LSJ) + \sum_{i=1}^{5}\left[\Delta E_{QED}(n_i l_i j_i, LSJ) + \Delta E_{HO}(n_i l_i j_i, LSJ)\right]. \quad (8)$$

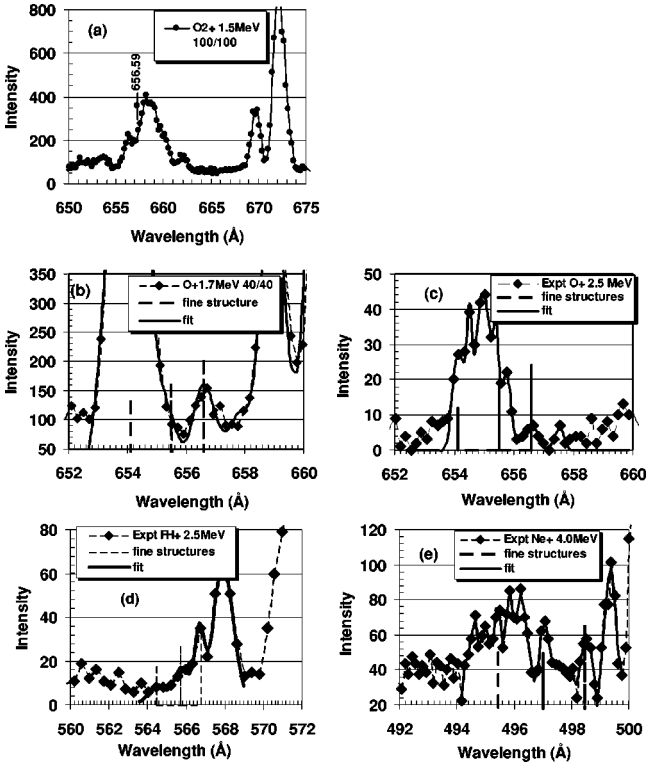

FIG. 2. The beam-foil spectra of the elements oxygen, fluorine, and neon recorded at different energies. The beam energies and spectrometer slit widths (in μm) are indicated.

B. The multiconfiguration Dirac-Fock method

We also used the MCDF [5,6] program to calculate the energies, lifetimes and relevant E1 transition rates of the three doubly excited sextet states $1s2s2p^3\ ^6S^o$, $1s2s2p^2 3s\ ^6P$, and $1s2p^3 3s\ ^6S^o$ of boronlike O IV, F V, and Ne VI. First, we used the single-configuration Dirac-Fock approach (SCDF). A basis of jj-coupled states with all possible total angular momenta J from two nonrelativistic configurations, such as $1s2s2p^3$ and $1s2s2p^2 3s$ or $1s2s2p^2 3s$ and $1s2p^3 3s$, was considered. After calculating all possible levels for all J, the eigenvectors were regrouped in the basis of the LS terms. To obtain better evaluation of the correlation energies of the three doubly excited sextet states $1s2s2p^3\ ^6S^o$, $1s2s2p^2 3s\ ^6P$, and $1s2p^3 3s\ ^6S^o$ in O IV, F V, and Ne VI, the improved calculations included $1s^2 2s^2 2p$, $1s^2 2s^2 2p^1$, $1s2s2p^3$, $1s2s2p^2 3s$, $1s2s2p^2 3p$, $1s2s2p^2 3d$, $1s2p^3 3s$, $1s2p^3 3p$, $1s2p^3 3d$, and $1s2p^3 4s$ mixing nonrelativistic configurations.

In the GRASP code [5,6] the QED effect, the self-energy, and the vacuum polarization correction are taken into ac-

TABLE I. The energies (in cm^{-1}) and wavelengths (in Å) for the $1s2s2p^2 3s\ ^6P_J - 1s2p^3 3s\ ^6S^o$ transitions in O IV, F V, and Ne VI by this work. Here we also list the QED and higher-order corrections for the $1s2s2p^2 3s\ ^6P_J - 1s2p^3 3s\ ^6S^o$ transitions in O IV, F V, and Ne VI. The errors for calculations are explained in the text.

Z	J	Experiment	E_{SCHF}	E^T_{SCHF}	E_{MCHF}	E^T_{MCHF}	E_{SCDF}	E_{MCDF}		Units
			±188	±107	±549	±531	±4172	±629		cm^{-1}
8	Av	152 519±23	152 175.4	152 280.7	151 885.8	152 034.3	149 538.7	152 091.9		cm^{-1}
		655.66±0.10	657.14	656.68	658.39	657.75	668.72	657.50		Å
				−22.9		−23.8			E_{QED}	cm^{-1}
				128.2		172.3			E_{HO}	cm^{-1}
	7/2	152 302±19	152 036.2	152 153.3	151 746.9	151 788.7	149 547.1	151 879.1		cm^{-1}
		656.58±0.08	657.74	657.23	658.99	658.81	668.69	658.42		Å
				−22.9		−23.8			E_{QED}	cm^{-1}
				139.9		65.7			E_{HO}	cm^{-1}
	5/2	152 505±23	152 196.8	152 410.6	151 907.4	152 034.1	149 770.8	152 147.0		cm^{-1}
		655.50±0.10	657.04	656.12	658.30	657.75	669.47	657.26		Å
				−22.9		−23.8			E_{QED}	cm^{-1}
				236.6		150.5			E_{HO}	cm^{-1}
	3/2	151 901±23	152 421.7	152 753.5	152 131.4	152 280.4	149 770.8	152 434.9		cm^{-1}
		654.02±0.10	656.07	654.65	657.33	656.68	667.69	656.02		Å
				22.9		−23.8			E_{QED}	cm^{-1}
				354.6		172.8			E_{HO}	cm^{-1}
9	Av	176 747±47	176 543.0	176 595.5	176 399.8	176 336.7	173 947.1	176 152.2		cm^{-1}
		565.78±0.15	566.43	566.27	566.89	567.10	574.89	567.69		Å
				−40.3		−42.6			E_{QED}	cm^{-1}
				92.8		−20.5			E_{HO}	cm^{-1}
	7/2	176 460±47	176 327.9	176 374.7	176 132.7	176 091.0	173 913.5	175 941.3		cm^{-1}
		566.70±0.15	567.13	566.97	567.75	567.89	575.00	568.37		Å
				−40.3		−42.6			E_{QED}	cm^{-1}
				87.1		0.9			E_{HO}	cm^{-1}
	5/2	176 832±47	176 651.4	176 860.5	176 455.3	176 223.2	173 916.4	176 190.7		cm^{-1}
		565.51±0.15	566.09	565.42	566.72	567.46	574.99	567.57		Å
				−40.3		−84.5			E_{QED}	cm^{-1}
				249.4		−147.6			E_{HO}	cm^{-1}
	3/2	177 198±47	177 049.1	177 268.4	176 851.3	176 736.0	174 060.3	176 516.4		cm^{-1}
		564.34±0.15	564.82	564.12	565.45	565.82	574.51	566.52		Å
				40.3		−84.5			E_{QED}	cm^{-1}
				259.6		−30.8			E_{HO}	cm^{-1}
10	Av	201 054±20	201 081.3	200 878.0	200 922.6	201 117.9	199 161.2	201 401.3		cm^{-1}
		497.38±0.05	497.31	497.81	497.70	497.22	502.11	496.52		Å
				−65.7		−71.6			E_{QED}	cm^{-1}
				−137.7		267.0			E_{HO}	cm^{-1}
	7/2	200 586±20	200 613	200 522.8	200 455.9	200 627.2	198 572.6	200 793.0		cm^{-1}
		498.54±0.05	498.47	498.70	498.86	498.44	503.59	498.03		Å
				−65.6		−71.6			E_{QED}	cm^{-1}
				−24.6		242.9			E_{HO}	cm^{-1}
	5/2	201 175±20	201 194.1	201 127.4	201 035.1	201 371.0	199 326.0	201 575.3		cm^{-1}
		497.08±0.05	497.03	497.20	497.43	496.60	501.69	496.09		Å
				−65.6		−142.0			E_{QED}	cm^{-1}
				−1.1		477.9			E_{HO}	cm^{-1}
	3/2	201 820±20	201 848.8	201 887.7	201 688.1	201 838.2	200 091.1	202 357.0		cm^{-1}
		495.49±0.05	495.42	495.32	495.82	495.45	499.77	494.18		Å
				−65.6		−142.0			E_{QED}	cm^{-1}
				104.6		292.2			E_{HO}	cm^{-1}

TABLE II. Fine structures (in cm^{-1}) of the $1s2s2p^2 3s\ ^6P_J$ state in O IV, F V, and Ne VI.

Z	Experiment	$SCHF^T$	$MCHF^T$	SCDF	MCDF	Experiment	$SCHF^T$	$MCHF^T$	SCDF	MCDF
	$J=7/2$-$5/2$					$J=5/2$-$3/2$				
8	254 ± 19	257	245	224	268	345 ± 19	343	246	174	288
				163					211	
9	371 ± 38	486	132	144	246	367 ± 38	408	513	3	325
				367					410	
10	589 ± 15	605	744	765	1161	646 ± 15	760	467	753	841
				655					687	

count by using the effective nuclear charge Z_{eff} in the formulas of QED, which come from an analogous hydrogenic orbital with the same expectation value of r as the MCDF orbital in question [5,6].

III. EXPERIMENT

The experiments were performed with the standard fast beam-foil excitation system on a 2-MeV Van de Graaff accelerator beam line at the University of Liege [10–13]. To produce the spectra of oxygen in the wavelength region near 500–1500 Å, the beam current of about 1.3 μA of $^{16}O^+$ and $^{32}O_2^+$ ions at beam energies between 1.2 and 1.7 MeV crossed a thin ($\sim 10\ \mu$ g/cm^2) exciter carbon foil. Light emitted at about 90° to the ion-beam direction was analyzed by a 1-m Seya-Namioka spectrometer, equipped with a low-noise channeltron detector; 25 spectra were recorded in the wavelength range around 500–1500 Å at slit widths of 100/100 and 40/40 μm. Through the use of optical refocusing spectroscopy, a full width at half maximum (FWHM) of 0.7 Å was achieved. Spectra in which the sextet lines in oxygen, fluorine, and neon were expected are available from some previous measurements. These yield information on wavelengths, intensities, and line shapes, and are very helpful for a comparison with our present calculations of the sextet states and the oxygen measurements. The spectra of O^{3+} and F^{4+} were recorded from beams of $^{16}O^+$ and $^{20}(FH)^+$ ions at an energy of 2.5 MeV with similar experimental procedures at the University of Lyon. Linewidths in the spectra are 0.4 Å and 0.8 Å. The spectrum of Ne^{5+} was produced and recorded from a beam of $^{20}Ne^+$ ions at the Argonne National Lab Dynamitron Accelerator, at an energy of 4 MeV. The spectrum was taken in the second grating order to help to identify and resolve the sextet spectrum. Linewidths are about 0.4 Å.

IV. RESULTS

The sextet transitions appear as weak lines among a rich collection of other unidentified lines of highly excited oxygen, fluorine and neon. Figure 2 shows five spectra recorded in the wavelength regions of interest. Initial peak locations were found using nonlinear least squared fits to Gaussian profiles. The wavelength measurement procedures and results for each set of transitions are described below in more detail.

A. $1s2s2p^2 3s\ ^6P - 1s2p^3 3s\ ^6S^o$ transitions in O IV

We obtained spectra at several different ion beam energies in the wavelength region where the sextet transitions $1s2s2p^2 3s\ ^6P - 1s2p^3 3s\ ^6S^o$ in O IV were expected. Three typical spectra at different energies are shown in Figs. 2(a), 2(b), and 2(c). A promising candidate for the transition at 656.58 ± 0.08 Å remains in the spectra at 1.7 and 2.5 MeV O^+ ion-beam energies, which is blended with a strong O III $2s^2 2p 3p\ ^3P - 2s2p^2 4f\ ^3D$ line in the spectrum at 1.2 MeV O_2^+ ion-beam energy. The $3d-4f$ and $3p-4d$ transitions of berylliumlike O V are seen at 654.72 Å and 659.60 Å in Fig. 2(c). The two wavelengths have been semiempirically fitted with an accuracy ±0.004 Å by [14–16] and provide a good calibration for our measurements. The standard error for wavelength calibration is 0.01 Å in the region of 650–670 Å. Nonlinear least square fits of Gaussian profiles gave the values for the wavelengths, intensities, and FWHM of lines. The uncertainties of the wavelengths are related to the intensities of the lines. The precision of the profile-fitting program was also checked through several known transition wavelengths. The fitted curves are shown in the Figs. 2(b) and 2(c).

For the $1s2s2p^2 3s\ ^6P_J - 1s2p^3 3s\ ^6S^o$ transitions, we expected to see the fine structures in our experiments. The strongest transition related to fine-structure components is the $J=7/2$–$5/2$ transition at the wavelength of 656.58 ± 0.08 Å. We also obtained the wavelength for the $J=5/2$–$5/2$ transition at 655.50 ± 0.10 Å. The $J=3/2$–$5/2$ transition at 654.02 Å is weak and blended with the strong $3d-4f$ transitions of O V at the ion energy of 1.7 MeV in Fig. 2(b), where it is hard to deconvolute the line out of the strong $3d-4f$ transitions and the relative intensities are difficult to compare. We obtained the wavelength of the $J=3/2$–$5/2$ transition of 655.50 ± 0.10 Å by fitting the spectrum at the energy of 2.5 MeV in Fig. 2(c). The transition rate is proportional to the area of the peak (the fitted intensity $\times$FWHM of the experiments). The ratio of the $J=7/2$-$5/2$ and $J=5/2$–$5/2$ transition rates at the ion energy of 1.7 MeV in Fig. 2(b) is found to be about $167\times0.7{:}124\times0.7 = 4.06{:}3$, and is consistent with the theoretical value 8:6 if we ignore other small differences. The ratio of the $J=7/2$–$5/2$, $J=5/2$–$5/2$, and $J=3/2$–$5/2$ transition rates at the energy of 2.5 MeV in Fig. 2(c) is about 7.7:5.9:4.0. Within an experimental error, these ratios are consistent with the theoretical values of 8:6:4. In Table I we present our measured fine-structure wavelength values and compare

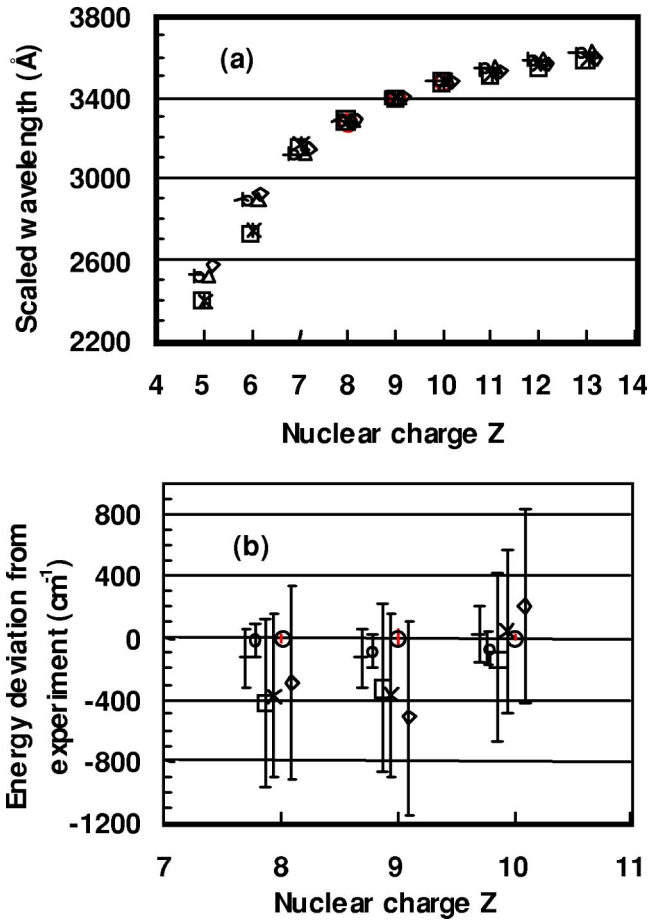

FIG. 3. (a) Scaled isoelectronic plot of the center of gravity of the wavelengths $\lambda(Z\text{-}3)$ and (b) transition energy deviations from experiment for the $1s2s2p^2 3s\,{}^6P\text{–}1s2p^3 3s\,{}^6S^o$ multiplet transitions for the boron sequence. The measured and calculated points are denoted by the following: circles with errorbars inside, ⊙ for experiments, + for SCHF, ○ for SCHFT, box for MCHF, * for MCHFT, △ for SCDF, and ♢ for MCDF.

them with our different theoretical values for O IV. The associated fine structures of the lower state $1s2s2p^2 3s\,{}^6P_J$ for $J=7/2\text{-}5/2$ and $J=5/2\text{-}3/2$ are 254 ± 19 cm^{-1} and 345 ± 19 cm^{-1}, respectively, listed in Table II, and are consistent with our calculations.

B. The $1s2s2p^2 3s\,{}^6P\text{–}1s2p^3 3s\,{}^6S^o$ Transitions in F V

Figure 2(d) shows the spectrum of $^{20}(FH)^+$ at a beam energy of 2.5 MeV recorded at Lyon, France. Many unidentified lines are located in the wavelength region where the sextet lines were expected. In addition, the $1s^2 4f\text{–}1s^2 6g$ transition of lithiumlike F VII at 535.52 Å and the $2s^2 2p^2\text{–}2s2p^3$ transitions of carbonlike F IV at 572.66 Å are observed. These wavelengths have previously been determined with an accuracy ±0.026 Å and ±0.003 Å [17,18] and help to provide a good calibration for our measurements. The same experimental procedures and programs described above were applied to analyze the spectrum for F V. The standard error for wavelength calibration is 0.03 Å in the region of 562–575 Å. The spectroscopic linewidths were about <0.8 Å. The fitted curve is shown in the Fig. 2(d).

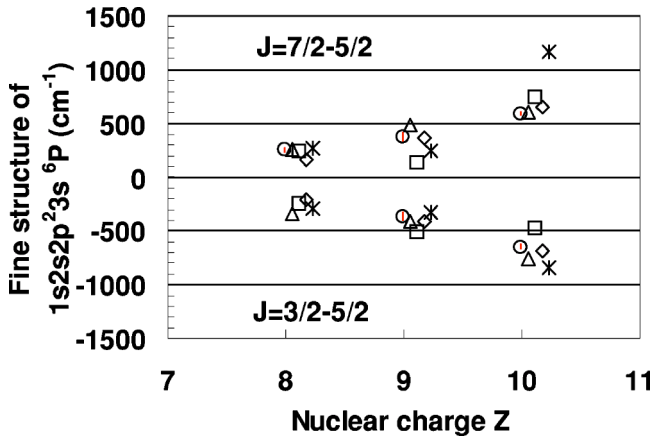

FIG. 4. Comparison of theexperimental (circles with errorbars inside ⊙) and theoretical fine structures for the $1s2s2p^2 3s\,{}^6P_J$ states in O IV, F V, and Ne VI. The calculated points are denoted by the following: △ for SCHFT, box for MCHFT, ♢ for SCDF, and * for MCDF.

For the $1s2s2p^2 3s\,{}^6P_J\text{–}1s2p^3 3s\,{}^6S^o$ transitions, we hoped to see the fine structures in our experiments. However, as shown in Fig. 2(d), the count rates of the expected lines in the wavelength region near 562–575 Å are slightly low. The wavelengths for the $J=7/2$, 5/2, 3/2–5/2 transitions are 566.70 ± 0.15 Å, 565.51 ± 0.15 Å, and 564.34 ± 0.15 Å, respectively, with slightly large errorbars. The ratio of the three transition rates is found to be about 7.8:5.9:4.0. It is consistent with the theoretical values of 8:6:4 within an precision. In Table I, we present our measured fine-structure wavelength values and compare these with our theoretical values for F V. The associated fine structures of the lower state $1s2s2p^2 3s\,{}^6P_J$ for $J=7/2\text{–}5/2$ and $J=5/2\text{–}3/2$ are 371 ± 38 cm^{-1}, and 367 ± 38 cm^{-1}, respectively, listed in Table II. These are consistent with our calculations.

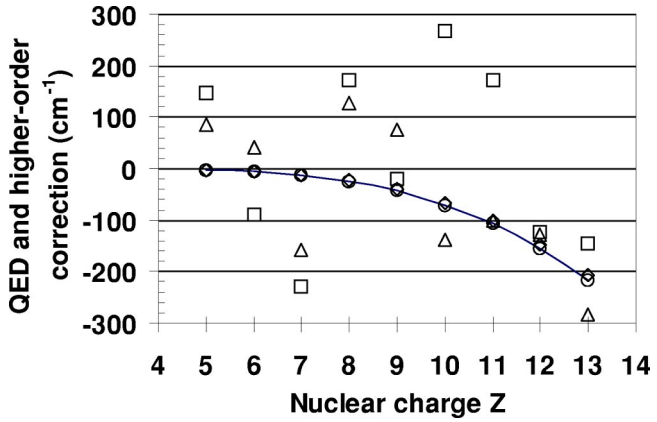

FIG. 5. Isoelectronic comparison of the QED effect and higher-order corrections of the $1s2s2p^2 3s\,{}^6P\text{–}1s2p^3 3s\,{}^6S^o$ transitions for the boron sequence. The calculated points are denoted by the following: ♢ for QED effects from SCHF, △ for higher-order corrections from SCHF, ○ for QED effects from MCHF, and box for higher-order corrections from MCHF. The fitted QED effect from both SCHF and MCHF are denoted by solid line.

TABLE III. Lifetimes (in ps) of the $1s2s2p^2 3s\ ^6P_J$ states and $1s2p^3 3s\ ^6S^o$ in O IV, F V, and Ne VI.

	This work				Others		
Z	SCHF	MCHF	SCDF	MCDF	Experiment [1]	MCDF [1]	MCHF [3]
	$1s2s2p^2 3s\ ^6P$						
8	221.13	118.76	306.39	182.81	99±12	125	144
9	118.46	61.44	159.93	85.93	73±15	64	71.22
10	70.09	42.48	92.07	47.70			
	$1s2p^3 3s\ ^6S^o$						
8	217.05	231.13	405.00	325.90			
9	185.05	312.29	330.48	269.97			
10	160.90	250.17	278.28	228.17			

C. The $1s2s2p^2 3s\ ^6P - 1s2p^3 3s\ ^6S^o$ transitions in Ne VI

The same experimental procedures and programs were applied to analyze the spectrum for Ne VI. Figure 2(e) shows the second order spectrum of neon from a beam of $^{20}Ne^+$ at an energy of 4 MeV. In the wavelength region where the sextet lines were expected, many unidentified lines are located as well as the nearby $1s4d$-$1s5f$ transition of helium-like Ne IX at 499.37 Å. The wavelength is known with an accuracy ±0.004 Å [19,20] and provides a good calibration for our measurements. The standard error for wavelength calibration is 0.02 Å in the region of 490-500 Å. The spectroscopic linewidths were about <0.4 Å. The fitted curve is shown in Fig. 2(e).

For the $1s2s2p^2 3s\ ^6P_J - 1s2p^3 3s\ ^6S^o$ transitions, we hoped to see the fine structures in our experiments. The wavelengths for the $J=7/2$, 5/2, 3/2-5/2 transitions are 498.54±0.05 Å, 497.08±0.05 Å, and 495.49±0.05 Å. The ratio of the three transition rates is found to be about 7.7:5.9:4.0, and is consistent with the theoretical value of 8:6:4 within experimental error. From the transition rates, we verify our identifications of the three transitions. In Table I, we present our measured fine-structure wavelength values and compare these with our theoretical values for Ne VI. The associated fine structures of the lower state $1s2s2p^2 3s\ ^6P_J$ for $J=7/2$–5/2 and $J=5/2$–3/2 are 589±15 cm^{-1}, and 646±15 cm^{-1}, respectively, as listed in Table II, and are consistent with our calculations.

V. COMPARISONS OF THE $1s2s2p^2 3s\ ^6P - 1s2p^3 3s\ ^6S^o$ TRANSITIONS WITH THEORY ALONG ISOELECTRONIC SEQUENCE

In Fig. 3(a), we show a plot of the center of gravity of the $1s2s2p^2 3s\ ^6P - 1s2p^3 3s\ ^6S^o$ transition wavelengths $\lambda(Z-3)$ for boronlike ions. The experimental results show a good consistency with the trend of the various calculations for $Z=5$–13. Detailed comparisons of the deviations of calculated transition energy from experimental values for O IV, F V, and Ne VI are shown in Fig. 3(b). The errorbars of the experiments are small and inside the circles. The errors shown in the first line of the Table I are the root mean square differences of the calculated and experimental values for the transition energies as given below in the table. The errors of the SCHF, SCHFT, MCHF, MCHFT, SCDF and MCDF energy calculations are ±188 cm^{-1}, ±107 cm^{-1}, ±549 cm^{-1}, ±531 cm^{-1}, ±4172 cm^{-1}, and ±629 cm^{-1}, respectively. Thus, by comparing the results in Fig. 3(b) and in Table I we can see (i) the single configuration interaction is the most important part of the all configuration interactions, (ii) the interactions between the configurations that we chose are effective to get more accurate results, and (iii) the sextet transition energies are sensitive to relativistic, electron correlation, and even QED effects, especially for heavy ions.

In Table II, we summarize the detailed results of the fine structures of the $1s2s2p^2 3s\ ^6P_J$ state for O IV, F V, and Ne VI. The comparison of the measured fine structures of the

TABLE IV. Electron screening σ for the $2s$ and sp valance electrons of the $1s2s2p^2 3s\ ^6P_J$ and $1s2p^3 3s\ ^6S^o_{5/2}$ states in O IV, F V, and Ne VI.

	$1s2s2p^2 3s\ ^6P_J$					$1s2p^3 3s\ ^6S^o_{5/2}$	
Z	SCHF				MCHF	SCHF	MCHF
	$J=7/2$	$J=5/2$	$J=3/2$	Av	Av	$J=5/2$	$J=5/2$
8	2.1577	2.1572	2.1565	2.1578	2.1362	2.6520	2.6290
9	2.1554	2.1545	2.1534	2.1535	2.1354	2.6380	2.6197
10	2.1524	2.1524	2.1496	2.1492	2.1357	2.6272	2.6145
Av	2.1552	2.1559	2.1549	2.1535	2.1357	2.6391	2.6211
Er	0.0026	0.0031	0.0035	0.0025	0.0002	0.0718	0.0425

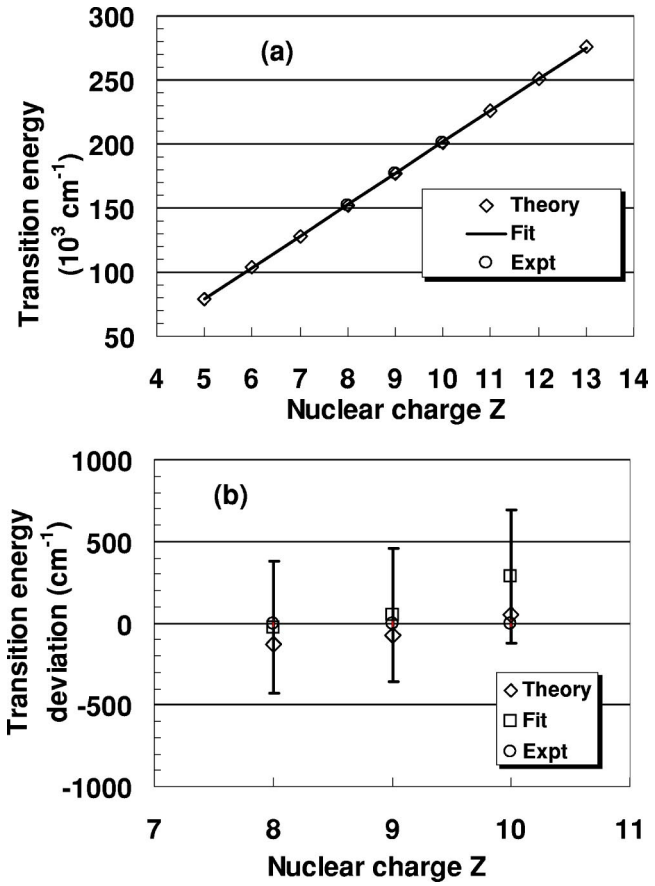

FIG. 6. Isoelectronic comparison of the theoretical and experimental mean wavelengths of the $1s2s2p^2 3s\,^6P$–$1s2p^3 3s\,^6S^o$ transitions for the boron sequence.

$1s2s2p^2 3s\,^6P_J$ state with theoretical values shows reasonable agreement (see Fig. 4). Here, the errorbars of experiments are also small and inside the circles.

The QED effects and higher-order corrections for the $1s2s2p^2 3s\,^6P$–$1s2p^3 3s\,^6S^o$ transitions in O IV, F V, and Ne VI are up to the 1.1–400 cm^{-1} level (see Table I) and cannot be ignored in careful comparisons with the experiments. Here the QED effects and higher-order corrections are calculated based on the Z_{eff} values from the SCHF and MCHF results. We plot the QED effects and higher-order corrections to the mean $1s2s2p^2 3s\,^6P$–$1s2p^3 3s\,^6S^o$ transition energies in Fig. 5. The QED effects increase with Z rapidly. The results show that the mean transition wavelengths are sensitive to the QED effects of 0.099 Å, 0.129 Å, and 0.17 Å for the $1s2s2p^2 3s\,^6P$–$1s2p^3 3s\,^6S^o$ transitions in O IV, F V, and Ne VI. These are at the same level or larger than our estimated experimental precision of ± 0.10 Å, ± 0.15 Å, and ± 0.05 Å.

Our MCHF calculated lifetime results for the upper $1s2s2p^2 3s\,^6P$ states for O IV, F V, and Ne VI agree with the measurements [1] and the calculations [1,3] within 20%, which is close to the experimental errors (see Table III). The MCDF and SCHF results are in fair agreement, which are two to three times of the experiments. The discrepancy between theory and experiments is most probably due to the additional decay modes of $M2$ and radiative autoionization or some missing configurations, which are important for MCHF and MCDF calculations. Although we do not have experimental values to compare, in Table III we also list our calculated lifetime results for the $1s2p^3 3s\,^6S^o$ states for O IV, F V, and Ne VI for future experiments.

Figure 6(a) shows a plot of the gravity center of the $1s2s2p^2 3s\,^6P$–$1s2p^3 3s\,^6S^o$ transition energy for boronlike ions versus nuclear charge Z. The diamonds are the weighted values of our different calculations. The solid line is a fit to the theoretical values. The circles are for experiments with errorbars inside. The fit expression is

$$\Delta E(\text{in } 10^3 \text{ cm}^{-1}) = A_0 + A_1 Z, \tag{9}$$

where $A_0 = -43.5635 \pm 0.6125$ and $A_1 = 24.5097 \pm 0.0654$.

Our measured transition energies for O IV, F V, and Ne VI are consistent with the trend of our different calculations shown in Fig. 6(a). The sextet states in boronlike ions are highly doubly excited (see Fig. 1), and the fine structures of the sextet states of the boronlike isoelectronic sequence are very similar. So the screened hydrogenlike calculation is a good approximation. For the same type of sextet states, the electron screening σ almost does not change with the nuclear charge Z (see Table IV). With $Z_{eff} = Z - \sigma$, the transition energy can be written as

$$\Delta E \simeq -\frac{1}{2}[(Z_{up})^2 - (Z_{lo})^2]$$

$$\simeq \frac{1}{4}(\sigma_{up} - \sigma_{lo})[2Z - (\sigma_{up} + \sigma_{lo})]. \tag{10}$$

We can see the linear relation. For more detail, Fig. 6(b) shows the deviations of the calculated (marked as diamonds) and the fitted (marked as squares) transition energies from the experiments for O IV, F V, and Ne VI. These are less than 300 cm^{-1}. Hence, the Eqs. (10) and (11) provide accurate energy approximations of the $1s2s2p^2 3s\,^6P$–$1s2p^3 3s\,^6S^o$ transitions in boronlike ions for $Z = 5$–13.

VI. CONCLUSIONS

The wavelengths and fine structures for the $1s2s2p^2 3s\,^6P_J$–$1s2p^3 3s\,^6S^o$ transitions in O IV, F V, and Ne VI have been investigated by the beam-foil spectroscopy and compared with the theoretical values obtained using the MCHF plus higher-order contributions and QED effect numerical calculations, and with the MCDF method. We have carefully studied the effect of configuration interaction, higher-order corrections, and QED effects on the energies, and relevant $E1$ transition energies and wavelengths. Agreement for the energies of the doubly excited sextet states $1s2s2p^2 3s\,^6P_J$ and $1s2p^3 3s\,^6S^o$ and their fine structures is satisfactory. We have also studied the effect of the configu-

ration interaction on the transition probabilities and lifetimes. For the lifetimes for the $1s2s2p^2 3s\ ^6P$ states in O IV and F V there remain large discrepancies of about 20% between our MCHF and MCDF calculations and experiments from Ref. [1]. The quantum electrodynamic and higher-order relativistic corrections are significant. Thus, the system provides a stringent test of *ab initio* theory, and allows differentiations to be made among various theoretical approaches.

[1] J.H. Blanke, B. Fricke, P.H. Heckmann, and E. Träbert, Phys. Scr. **45**, 430 (1992).
[2] L. Lapierre and É.J. Knystautas, J. Phys. B **33**, 2245 (2000).
[3] G. Miecznik, T. Brage, and C.F. Fischer, Phys. Scr. **45**, 436 (1992).
[4] C.F. Fischer, T. Brage, and P. Jonsson, *Computational Atomic Structure an MCHF Approach* (Institute of Physics Publishing, Bristol, 1997).
[5] F.A. Parpia, C.F. Fischer, and I.P. Grant, Comput. Phys. Commun. **94**, 249 (1996).
[6] S. Fritzsche and I.P. Grant, Comput. Phys. Commun. **103**, 277 (1997).
[7] K.T. Chung, X.W. Zhu, and Z.W. Wang, Phys. Rev. A **47**, 1740 (1992).
[8] K.T. Chung and X.W. Zhu, Phys. Rev. A **48**, 1944 (1993).
[9] G.W.F. Drake and R.A. Swainson, Phys. Rev. A **41**, 1243 (1990).
[10] A.E. Kramida, T. Bastin, E. Biemont, P.D. Dumont, and H.P. Garnir, J. Opt. Soc. Am. B **16**, 1966 (1999).
[11] H.G. Berry, R.L. Brooks, K.T. Cheng, J.E. Hardis, and W. Ray, Phys. Scr. **42**, 391 (1982).
[12] J.E. Hardis, H.G. Berry, L.G. Curtis, and A.E. Livingston, Phys. Scr. **30**, 189 (1984).
[13] H.P. Garnir, Y. Baudinet-Robinet, and P.D. Dumont, Nucl. Instrum. Methods Phys. Res. B **31**, 161 (1988).
[14] K. Bockasten and K.B. Johansson, Ann. Geophys., Ser. B **38**, 563 (1968).
[15] S.G. Pettersson, Phys. Scr. **26**, 296 (1982).
[16] C.E. Moore, NSRDS-NBS 3 Section 1-10 (1965-1983).
[17] C.E. Moore, Circ. Natl. Bur. Stand. **1**, 467 (1949).
[18] L. Engström, Phys. Scr. **29**, 113 (1985).
[19] R.T. Brown, Astrophys. J. **158**, 829 (1969).
[20] L.A. Vainshtein and U.I. Safronova, Phys. Scr. **31**, 519 (1985).